eLife

Reviewed Preprint
v1 • July 17, 2026
Not revised

For correspondence:
sangwoos@buffalo.edu

* These authors contributed equally to this work.

Funding: See page 11

Reviewing editor: Babak Momeni, Boston College, United States

Stabilizing by steering: Enhancing bacterial motility by non-uniform diffusiophoresis

Viet Sang Doan*, Ali Nikkhah*, Sangwoo Shin

Department of Mechanical and Aerospace Engineering, University at Buffalo, The State University of New York, Buffalo, United States

eLife Assessment

This study sets out to show that the directionality of bacterial transport in confined environments is affected by a salt gradient. Using Pseudomonas putida in microfluidics devices, the authors hypothesize that salt-induced diffusiophoresis acts as a steering mechanism to guide microbial movement. However, the evidence to support this hypothesis is **incomplete**, because the underlying reorientation process is not directly demonstrated, and the necessary controls to rule out alternative hypotheses are not presented.

https://doi.org/10.7554/eLife.111881.1.sa3

Abstract

Bacteria often traverse confined spaces to perform critical functions in symbiosis, infection, drug delivery, and soil bioremediation. While the canonical run-and-tumble strategy enables exploration, its reliance on constant sensing and stochastic reorientation limits efficiency under confinement. We show that salt gradients can physically steer *Pseudomonas putida* by biasing their runs toward salt through asymmetric diffusiophoretic forces. These gradients impose a torque strong enough to overcome Brownian rotation, aligning cells along the gradient and producing straighter, more persistent motion. We further show that when toxic organic contaminants are present, salt gradients enhance bacterial dispersion toward them, demonstrating improved chemotactic transport. This work uncovers a previously unrecognized mechanism by which salt gradients direct bacterial motility, revealing a physical route to control microbial transport and colonization in complex environments.

Introduction

Bioaugmentation is an soil bioremediation process in which cultured bacteria are introduced into contaminated soil to degrade pollutants [1]. Among numerous factors that determine the process efficacy, a critical prerequisite that is often challenging to achieve is to disperse the cells to the pollutant source, particularly to low permeability zones that are abundant in heterogeneous, unsaturated soil [2]. A successful bioaugmentation thus requires directing decomposer bacteria to the target soil micropores deep in the subsurface where the contaminants are present [3, 4]. While bacteria can passively advect across permeable regions of the subsurface via hydrodynamic dispersion, impervious areas, which are prevalent in heterogeneous soil matrix, can only be accessed by their active motility or Brownian motion. These areas often carry a significant amount of contaminants since they cannot be easily displaced hydrodynamically, thus limiting the effectiveness of remediation [5, 6].

The fact that decomposer bacteria can thrive on toxic contaminants makes them naturally chemotactic toward these contaminants [7–9]. In fact, it is well known that chemotaxis directs cells to pollutant-rich regions and improves bacterial retention during inoculation, implying active

migration toward low-permeability zones where contaminants tend to persist [10–13]. Nevertheless, the inherently stochastic nature of flagellar motility (*e.g.*, run-and-tumble) may limit the efficiency of this navigation [14, 15]; thus, rather deterministic transport mechanisms may offer more reliable targeting. Here, we hypothesize that *diffusiophoresis* could provide this deterministic guidance, enabling more directed bacterial migration toward contaminant-rich regions.

Diffusiophoresis describes the directed motion of colloidal particles along solute gradients, where the particle velocity can be precisely controlled by manipulating solute gradients [16]. A number of recent studies have shown that diffusiophoresis can be used to control colloidal transport in confined spaces, *e.g.*, porous media [17–23] and impervious dead-ends [24–30], as such regions typically display diffusion-limited environments. Also, the native surface charge of cell membranes makes bacteria susceptible to experiencing diffusiophoresis [31–33], although it remains elusive how diffusiophoresis affects flagellar motility. Motivated by these prior studies, here we investigate the impact of diffusiophoresis on the motility of soil bacterium, *Pseudomonas putida* F1, and demonstrate the use of diffusiophoresis in enhancing chemotactic dispersion toward non-aqueous phase liquid (NAPL) in confined geometries.

Results

Salt Gradients Induce Directional Cell Migration

To observe the motility of *P. putida* F1 under the influence of salt gradients, we use a transparent microfluidic device consisting of two parallel flow channels connected by a narrow pore (Figure 1a). One end of the pore is sealed with a thin hydrogel membrane (polyethylene glycol diacrylate) to suppress undesired convective flows [34]. The membrane allows the diffusion of solute molecules, enabling the formation of stable salt gradients. Additional details on the fabrication process are provided in the SI and also in our previous work [35].

Initially, cells suspended in a 10 ×-diluted random motility buffer (11.2 g/L K_2HPO_4, 4.8 g/L KH_2PO_4, and 0.029 g/L EDTA) supplemented with 0.1 M NaCl are introduced into the open-sided flow channel (left channel in Figure 1a), while the same buffer containing 0.1 M NaCl is simultaneously injected into the gel-sided flow channel (right channel). Bacteria from the left flow channel swim into the pore, eventually achieving an even distribution across the pore after one hour (upper panel in Figure 1a). Then, a cell suspension at reduced salt concentration (1 mM NaCl with dilute motility buffer) is injected into the left flow channel to create salt gradients across the pore (lower panel in Figure 1a).

Upon the introduction of NaCl gradients, we observe that the overall cell population in the pore changes over time. As presented in Figure 1b, the total number of cells in the pore gradually increases in the presence of NaCl gradients, whereas the cell population remains nearly unchanged when the NaCl concentration is uniform throughout the channel. Moreover, not only does the total cell population increase, but also their spatial distribution changes, as shown in Figures 1c,d; the color code represents local number of cells normalized by the total cell number at $t = 0$. While the overall cell distribution remains more or less the same in the absence of NaCl gradients (Figure 1c, Movie S1), with NaCl gradients the cells tend to locate deeper into the channel toward higher salt concentration (Figure 1d, Movie S2). These results suggest that salinity gradients can attract the bacteria into the deep pores and promote their dispersion toward higher salinity.

Directional Alignment and Biased Motility under Salt Gradients

To better understand the observed salt-tactic behavior, we evaluate the motility of individual cells by analyzing their trajectories. Sample trajectories (unfiltered) with or without NaCl gradients at different time windows over a period of 25 s are presented in Figures 2a,b, which also display more cell trajectories found deep in the pore over time under NaCl gradients (Figure 2b).

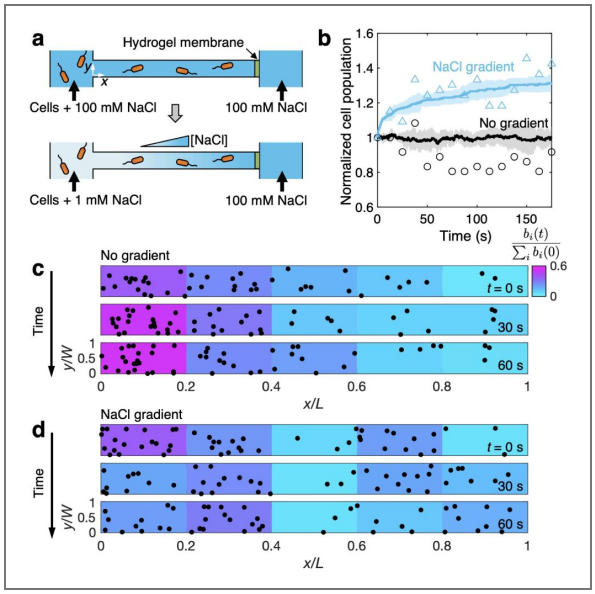

FIG. 1. ***P. putida*** **are attracted to higher salinity.**

(a) A microfluidic assay to evaluate cells under NaCl gradients. (b) Change in the total cell population normalized by the initial cell population over time in the presence (blue) and absence (black) of NaCl gradients. Symbols represent experimental data (blue triangles for NaCl gradients, black circles for no gradient) while solid lines represent numerical simulations. Shaded regions denote the standard deviation across three simulations. (c,d) Local distribution of cells over time (c) without (Movie S1) or (d) with NaCl gradients (Movie S2). The color code represents the number of cells in the *i*-th bin, $b_i(t)$, normalized by the total number of cells from the beginning, $\sum_i b_i(0)$. Although the heat map only shows one experiment here, the observed patterns were reproduced across multiple replicates, with similar trends

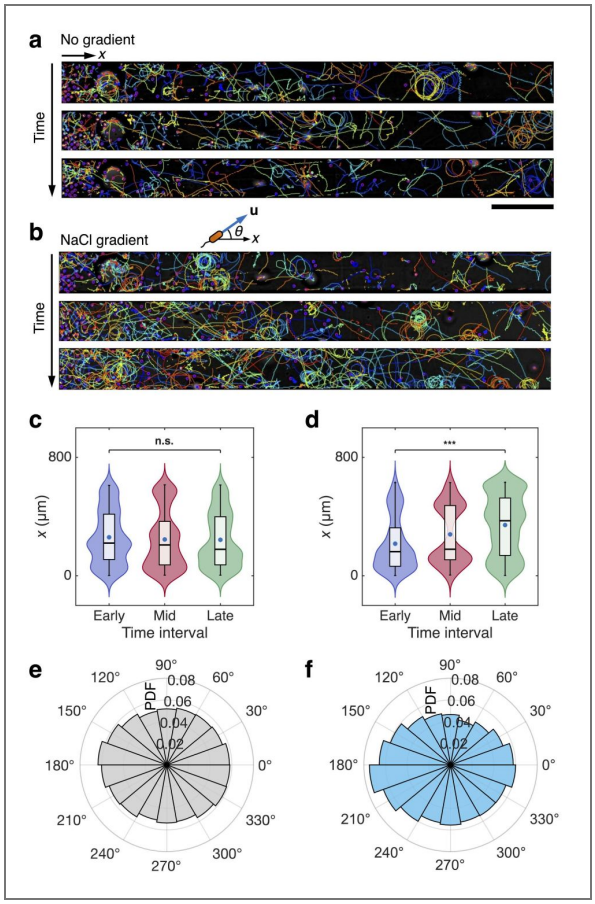

FIG. 2. ***P. putida*** **aligns along salt gradients.**

(a,b) Unfiltered cell trajectories recorded over 25 s of duration for different times (0–25, 75–100, 150–175 s) in the (a) absence and (b) presence of NaCl gradients. (c,d) Distribution of cell mean positions along the *x* axis at successive 25 s time intervals (Early: 0–25 s, Mid: 75–100 s, Late: 150–175 s) in the (c) absence and (d) presence of NaCl gradients. The white box in (c,d) indicates interquartile range with median shown as a stripe and mean as a dot. (e,f) Probability density function distribution of cell's directions of instantaneous velocity vectors in the (e) absence and (f) presence of NaCl gradients. Scale bar in (a) is 100 μm.

To quantitatively determine whether more cells move to the end of the pore, we analyzed the distribution of cell positions over time (Figure 2c,d). In the absence of NaCl gradients, the distribution remains spatially consistent, with no progressive shift in the position and distribution (Figure 2c). We did not observe any temporal change between early (0–25 s) and late (150–175 s) segments (Δx = -17.43 ± 18.9 μm, p = 0.36, n = 375 trajectories) [36]. In contrast, under NaCl gradients, the distribution shifts progressively deeper into the pore, as reflected by increases in the median and a broader distribution at later times extending toward larger x values (deeper into the pore), as shown in Figure 2d. The median position is increased from 216.9 ± 15.1 μm to 343.2 ± 19.6 μm (Δx = 126.30 ± 24.7 μm, p < 0.0001, n = 255 trajectories). More statistical details can be found in Table S1 (SI).

Upon analyzing the trajectories, we immediately identify that the cells tend to be more aligned along the salt gradient, where Figures 2e,f show the probability distribution of angle θ between the cell's instantaneous velocity vector u and the pore axis (+x direction). The slightly reduced distribution in the lateral direction ($\theta \to \pm 90°$) in the absence of NaCl gradients (Figure 2e) is likely due to the lateral confinement imposed by the slender geometry of the pore (width ≈ 65 μm). In the presence of NaCl gradients, the noticeable alignment toward the pore entrance ($\theta \to 180°$), i.e., away from the salt, is due to the run-and-reverse motility of *P. putida*, which is one of the pronounced motilities of lophotrichous *P. putida* [37–39]. Regardless of whether the cells are headed toward or away from the salt, the cells are aligned more along the pore direction (Figure 2f).

Next, we analyze their mean run speed, i.e., the average speed of the cell between successive tumble events. Here, we define 'tumble' as any sudden change in the cell speed and direction between two successive runs (Figure S1, SI). After processing over 1,412 runs combined, we did not observe any noticeable difference in the average run speed between the control group (no gradient) and the NaCl gradient cases (Figure 3a). However, when we plot the run speed in their corresponding directions (Figures 3b,c), we notice that there is a significant improvement in the run speed toward the salt ($\theta \to 0°$), and at the same time, the run speed decreases in the direction away from the salt ($\theta \to 180°$). We also note that we did not observe any significant difference in the tumble rates between the control and NaCl gradient cases (Figure 3h; Figure S2, SI), suggesting that NaCl gradients do not interfere with chemoreceptors [40].

While the observed bias in the run speed may be speculated as due to the additional diffusiophoretic drift toward salt, the speed change in fact cannot be explained by diffusiophoresis alone. Under current conditions, the diffusiophoretic velocity, $u_d \approx \mathscr{M}_d/\ell$ where $\mathscr{M}_d = \mathcal{O}(100\ \mu\text{m}^2/\text{s})$ is the diffusiophoretic mobility [32] and $\ell = \mathcal{O}(100\ \mu\text{m})$ is the characteristic length scale of the salt gradient, is estimated to be no more than 1 μm/s, which is an order of magnitude smaller than the measured speed change. Another possibility of the observed bias may be due to chemokinesis, which is a non-directional response in which cells modulate their swimming speed in response to local chemical concentration [41]. This behavior has been reported in uniform attractant concentrations without gradients, e.g., in *Rhodobacter sphaeroides Escherichia coli* and *Azospirillum brasilense* [42–44]. We analyze the instantaneous run speed of the bacteria and found no significant differences between 1 mM and 100 mM NaCl concentrations. Nonetheless, the difference was markedly significant (p < 0.001) under the salt gradients, as illustrated in Figure 3d. More statistical analysis can be found in Table S2 (SI). Therefore, we conclude that the observed bias in the run speed cannot be fully explained by chemokinesis.

Interestingly, as we observe how cells run by analyzing the straightness of each run, we notice that cells tend to run straighter toward the salt (Figures 3e-g). The run straightness, $\mathcal{S} = |x_k - x_1| / \sum_{j=1}^{k-1} (|x_{j+1}| - |x_j|)$, where x_j is the cell position at j-th frame within a single run, which is defined as the ratio of the end-to-end distance to the total distance the cell has traveled within a run, represents an effective tortuosity of runs [45, 46]. As shown in Figure 3g, the run straightness is noticeably improved when swimming toward the salt. This was unexpected since run straightness is mainly affected by the Brownian rotation or the inherent asymmetry of the cell, both of which are sensitive to the cell morphology [47].

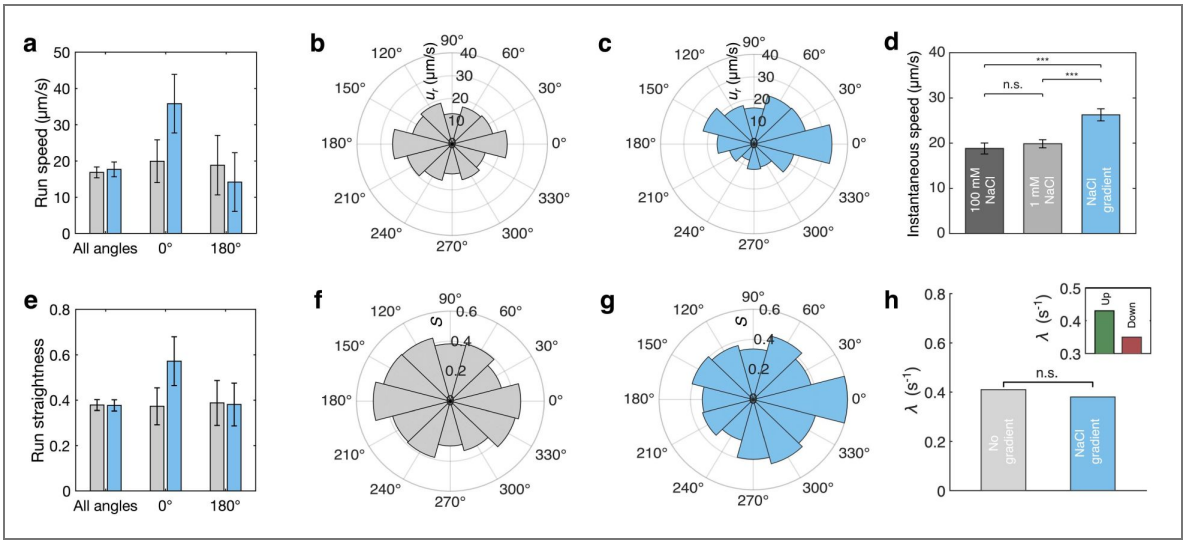

FIG. 3. ***P. putida*** **run faster and straighter toward salt.**

(a) Comparison of run speeds averaged over the entire angles, 0° (-15° < θ < 15°), and 180° (165° < θ < 195°). (b,c) Distributions of average run speed in the (b) absence and (c) presence of NaCl gradients. (d) Instantaneous run speed in the absence and presence of NaCl gradients (e) Comparison of average run straightness for entire angles, 0° (-15° < θ < 15°), and 180° (165° < θ < 195°). (f,g) Distributions of average run straightness in the (f) absence and (g) presence of NaCl gradients. (h) Tumble rates measured in the absence and presence of NaCl gradients. The inset compares tumble rates for runs oriented up gradient and down gradient. Error bars in (a, d, e) represent standard deviation.

P. putida is a lophotricous cell, *i.e.*, multiple flagella (length f ~ 5 μm, thickness ~ 20 nm) are attached at one end of the cell body (body length a ~ 1.5 μm, body width b ~ 0.8 μm) [37, 48]. Therefore, when *P. putida* propels forward the flagella tuft bundles up and forms a long, slender helix that is attached to the rod-like body where the body and the flagellar bundle are spatially segregated [49]. Given the asymmetry of this geometry, we hypothesize that the improved straightness toward the salt is due to *non-uniform diffusiophoresis* acting distinctly on the cell body and flagellar bundle.

Non-uniform Diffusiophoresis Steers Cells

Under the influence of salt gradients, the surface charge of the cell membrane triggers bacterial diffusiophoresis [32]. However, because there is a significant difference in the size and surface charge between the body (mainly consists of lipopolysaccharides and phospholipids) and the flagella (consist of flagellin), we expect that diffusiophoresis will not be occurring uniformly over the entire cell owing to the size- and charge-dependent nature of diffusiophoresis [25, 50–54]. As the cell body is larger and more charged than flagella, the body is expected to experience stronger diffusiophoresis. We confirm that the surface charge of the flagella is much smaller than the cell body, where the measured zeta potential of flagella isolated from the cell body is -0.6 ± 1.0 mV whereas the entire body is -16.3 ± 0.6 mV (SI). Considering the size and surface charge, the diffusiophoretic mobility of the body and flagellar bundle are estimated to be $\mathscr{M}_d^{\mathrm{body}} = 99.2\mu\mathrm{m/s}^2$ and $\mathscr{M}_d^{\mathrm{flag}} = 2.8\mu\mathrm{m/s}^2$, respectively [25, 50].

Therefore, when a cell swims toward salt, such an asymmetric action of diffusiophoresis tilts the cell body to align with the gradient (Figure 4a). This biased steering restores orientation along the gradient, stabilizes the trajectory, and enhances run speed by producing straighter paths.

To assess whether the rotation due to diffusiophoresis can overcome Brownian rotation, we evaluate the rotational Péclet number,

$$\mathrm{Pe_r} = \frac{2\Delta u_d}{(a+f)\,D_r} \sim \frac{2\pi\eta\Delta\mathscr{M}_d}{3kT\ell}\cdot\frac{(a+f)^2}{\ln\left(2\,(a+f)/b\right)-1/2}, \tag{1}$$

where $\Delta u_d = u_d^{\mathrm{body}} - u_d^{\mathrm{flag}}$ and $\Delta\mathscr{M}_d = \mathscr{M}_d^{\mathrm{body}} - \mathscr{M}_d^{\mathrm{flag}}$ are the diffusiophoretic velocity and mobility difference between the body and the flagella bundle, respectively, and $D_r = \frac{3kT}{\pi\eta}$. $\frac{\ln(2(a+f)/b)-1/2}{(a+f)^3}$ is the rotational diffusivity of the body plus flagella bundle [55]. We estimate $\mathrm{Pe_r}$ ~ 10, suggesting that such a subtle diffusiophoretic motion is yet powerful enough to overcome Brownian rotation, leading to improved motility toward salt. As shown in Figures 4b,c (Movies S3,S4), the run trajectories repositioned to start at the origin (x_0 , y_0) = (0, 0) indeed show the steering of cells toward the salt with straighter runs, confirming the impact of salt gradients on cell motion.

Cell steering due to diffusiophoresis can be further characterized by correlating the change of body angle $\Delta\theta$ over its arc length s along individual run trajectories, i.e., $\langle\cos(\Delta\theta)\rangle_s$, where $\langle\cdot\rangle_s$ is the ensemble average over all segments pairs with equal arc length separation across entire run trajectories (SI). As shown in Figure 4f, in the absence of salt gradients, the angle correlation decays slowly along its displacement, indicating persistent swimming along its initial direction within a run. In contrast, under salt gradients, the angle correlation decays faster, indicating increased directional decorrelation over its run path. This long-range decay is not attributed to any change in the rotational Brownian noise; rather, it arises from continuous, deterministic reorientation of the swimming direction enabled by the diffusiophoretic torque. Such forced steering introduces long-range curvature into the run trajectories, leading to a faster decay of angle correlation as the motion becomes globally biased toward the salt gradient.

Further analyzing the mean square displacement (MSD) of the run trajectories reveals that the observed long-range steering arises mainly from the change of cell motion along the gradient direction (SI). The MSD anisotropy, which is defined as the ratio of MSD components along the gradient direction ($\mathrm{MSD}_{||}$) and transverse to the gradient direction ($\mathrm{MSD}_{\perp}$), i.e., $\mathrm{MSD}_{||}/\mathrm{MSD}_{\perp}$. In

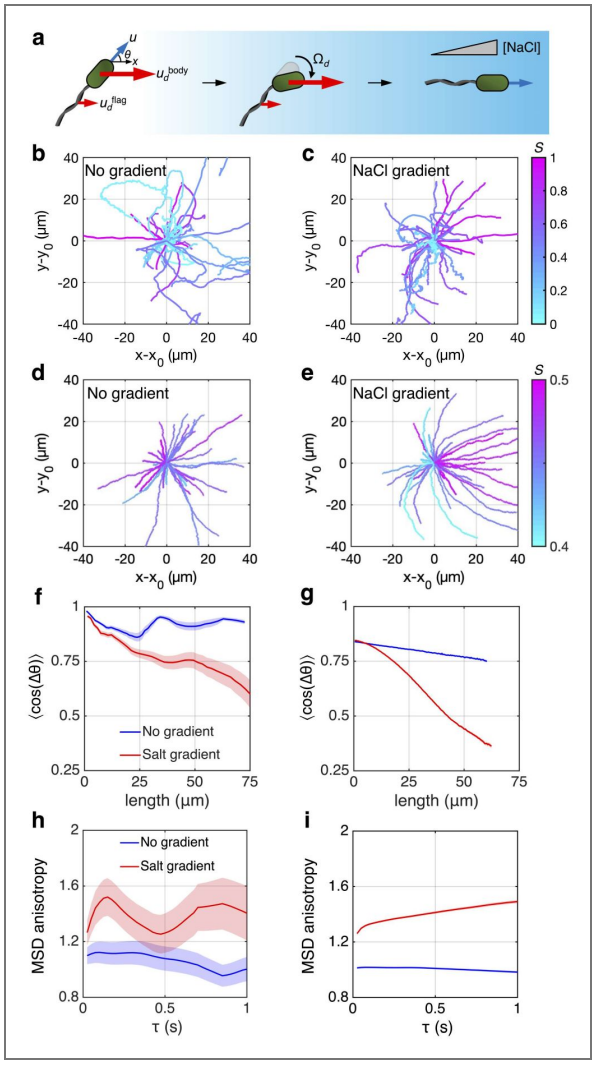

FIG. 4. Non-uniform diffusiophoresis steers *P. putida* toward salt.

(a) An illustration of cell rotation due to non-uniform diffusiophoresis. (b,c) Experimental run trajectories (40 randomly chosen) repositioned to start at the origin in the (b) absence (Movie S3) and (c) presence (Movie S4) of NaCl gradients. The color code represents run straightness S . (d,e) Numerical simulation run trajectories repositioned to start at the origin in the (d) absence (Movie S5) and (e) presence (Movie S6) of diffusiophoretic drift. (f,g) Angle correlation function $\langle\cos(\Delta\theta)\rangle$ in (f) experimental run trajectories and (g) simulation run trajectories. Shaded regions indicate ± standard error of the mean (SEM.) (h,i) MSD anisotropy ratio for (h) experimental run trajectories and (i) simulation run trajectories.

the absence of salt gradients, as shown in Figure 4h, the MSD anisotropy remains approximately unity across all lag times τ. However, under salt gradients, the MSD anisotropy is substantially increased, suggesting that the directional persistence is enhanced only along the gradient axis. Also, the MSD anisotropy is large even at very short lag times, indicating that the reorientation driven by diffusiophoretic torque occurs continuously throughout the entire run.

This result is fully consistent with the angle correlation analysis, where the correlation function decays much faster under salt gradients compared to the no-gradient conditions. Moreover, the elevated MSD anisotropy at the shortest lag times, together with the rapid decay of $\langle\cos(\Delta\theta)\rangle$, provides a clear signature of continuous orientation rather than biased run-time modulation characteristic of chemotaxis. The absence of any significant and noticeable change in the mean run time between the no-gradient and salt gradient conditions (Figure 3h and Figure S2) further rules out salt-taxis or chemotactic mechanisms, supporting non-uniform diffusiophoresis as the origin of the observed behavior here in this study. Comprehensive statistical analysis, including permutation tests for the MSD anisotropy, confirms the robustness of these findings (Table S3, SI).

The diffusiophoresis-driven steering can also be simulated by solving Langevin equations for cell translation and rotation (SI). The rotation of Brownian cell subject to diffusiophoresis can be modeled as $\dot{\theta}(t) = \Omega_d + \eta_r(t)$, where $\Omega_d = \frac{2\Delta u_d}{a+f}\sin\theta$ is the rotation due to non-uniform diffusiophoresis, and $\eta_r(t)$ is the random Brownian rotation. The simulation results are shown in Figures 4e where NaCl gradients effectively steer the cells toward salt and enable straighter runs, displaying a qualitative agreement with the experimental trajectories shown in Figure 4c. The non-uniform diffusiophoresis also yields the rapid decay in the angle correlation (Figure 4g) and the increased MSD anisotropy (Figure 4i). Furthermore, the simulations also predict the change in the global (Figure 1b) and local (Figure S3) cell population under the impact of nonuniform diffusiophoresis, which is consistent with the experimental results shown in Figures 1b and 2b.

Diffusiophoresis Enhances Bacterial Dispersion toward Pollutants

Finally, we evaluate the diffusiophoretic cell dispersion in the presence of NAPL; toluene. While toluene is highly toxic to most microorganisms due to its membrane-disrupting effects, *P. putida* is resistant and capable of metabolizing toluene, which drives its natural chemotaxis toward the compound [56–59]. Using the same microfluidic device, we inject *P. putida* suspended in low salinity water (1 mM NaCl) into a channel that is initially filled with high salinity water (0.1 M NaCl) while toluene is present in the gel-sided flow channel (Figures 5a,b), effectively simulating diffusiophoresis-enabled bioaugmentation of NAPL-contaminated subsurface. Toluene gradually dissolves and creates toluene gradients in addition to salt gradients, creating dual chemical gradients.

In the presence of toluene, we observe that cells initially chemotax toward toluene, but soon after they slow down due to the toxicity at high toluene concentration [60, 61], making it challenging to disperse cells closer to the contaminant source (Figure 5c, Movie S7). On the other hand, when NaCl gradients are additionally imposed, the cells continuously migrate into the pore via diffusiophoresis despite the lack of flagellar motility, as diffusiophoresis is forcing the cells to move toward the contaminant source (Figure 5d, Movie S8). This demonstration suggests the potential utility of diffusiophoresis for bioremediation of NAPL-contaminated soil using externally imposed salt gradients.

Conclusion

Our results indicate that diffusiophoresis can improve the swimming motility of *P. putida* to reach targets in confined geometries, offering a promising strategy for bioremediation in contaminated soil environments. While this work only focuses on *P. putida*, we expect other similar lophotrichous cells to experience similar diffusiophoresis-enhanced motility improvement due to the asymmetric geometry of the cell and the native surface charge of bacterial membranes [32]. In

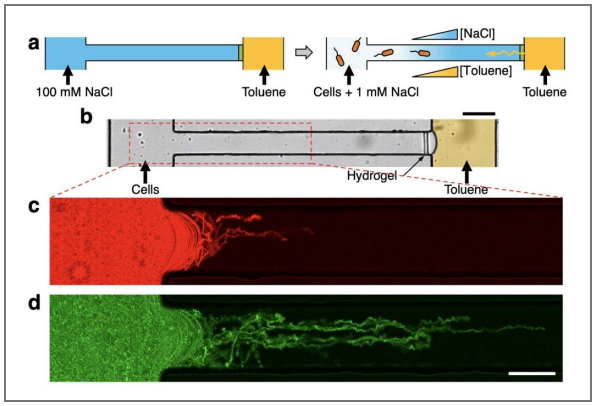

FIG. 5. Salt gradients disperse cells toward toxic contaminant.

(a) Simulating diffusiophoretic bioaugmentation of toluene-contaminated pore. Cells suspended in low salinity water are injected into the channel that is filled with high salinity water in the presence of toluene on the gel-sided channel, thereby creating dual chemical (salt and toluene) gradients. (b) An image of the microfluidic channel in the presence of toluene. Toluene is false-colored. (c,d) Trajectories of cells in the (c) absence (Movie S7) and (d) presence of NaCl gradients. (Movie S8) Scale bars in (b,d) are 50 μm.

the same reasoning, we expect that peritrichous cells (e.g., *Escherichia coli*) are likely to experience the diffusiophoresis-induced steering much less since their body and flagella are not spatially separated, unlike lophotrichous cells. This warrants further investigations to uncover how flagellar configuration determines cellular diffusiophoresis.

Data availability

All codes, data files, and documentation for tracking can be accessed via the GitHub repository *https://github.com/alinikkh/-Pseudomonas-putida-F1-tracking*.

Acknowledgements

This material is based upon work supported by the National Science Foundation under Grants No. 2223737 and 2237177.

We thank Drs. Roseanne Ford and Rhea Braun for providing *P. putida*.

Additional information

Author Contributions

Conceptualization: S.S.; Methodology: V.S.D., and A.N.; Investigation: V.S.D., and A.N.; Resources: S.S.; Writing–original draft: all authors; Writing–reviewing and editing: all authors; Funding acquisition: S.S.

Funding

Funder	Grant reference number	Author
National Science Foundation (NSF)	2223737	Sangwoo Shin
National Science Foundation (NSF)	2237177	Sangwoo Shin

Author ORCID iDs

Sangwoo Shin: https://orcid.org/0000-0001-5618-8522

Additional files

Supplementary material.

Movie S1.

Movie S2.

Movie S3.

Movie S4.

Movie S5.

Movie S6.

Movie S7.

Movie S8.

References

[1] **Vogel TM** (1996) Bioaugmentation as a soil bioremediation approach. *Current opinion in biotechnology* **7**:311 https://doi.org/10.1016/s0958-1669(96)80036-x | PubMed

[2] **Lyon DY,** Vogel TM (2012) Bioaugmentation for groundwater remediation: an overview. In: Stroo H, Leeson A, Ward C (Eds). *Bioaugmentation for Groundwater Remediation* pp. 1-37 https://doi.org/10.1007/978-1-4614-4115-1_1

[3] **Pieper DH,** Reineke W (2000) Engineering bacteria for bioremediation. *Curr. Opin. Biotechnol.* **11**:262 https://doi.org/10.1016/s0958-1669(00)00094-x | PubMed

[4] **Yang P,** van Elsas JD (2018) Mechanisms and ecological implications of the movement of bacteria in soil. *Appl Soil Ecol* **129**:112 https://doi.org/10.1016/j.apsoil.2018.04.014

[5] **Sturman PJ,** Stewart PS, Cunningham AB, Bouwer EJ, Wolfram JH (1995) Engineering scale-up of in situ bioremediation processes: a review. *J. Contam. Hydrol* **19**:171 https://doi.org/10.1016/0169-7722(95)00017-p

[6] **Alexander M** (1999) *Biodegradation and Bioremediation* Gulf Professional Publishing.

[7] **Harwood CS,** Rivelli M, Ornston LN (1984) Aromatic acids are chemoattractants for pseudomonas putida. *J. Bacteriol* **160**:622 https://doi.org/10.1128/jb.160.2.622-628.1984 | PubMed

[8] **Law AM,** Aitken MD (2003) Bacterial chemotaxis to naphthalene desorbing from a nonaqueous liquid. *Appl Environ Microbiol* **69**:5968 https://doi.org/10.1128/AEM.69.10.5968-5973.2003 | PubMed

[9] **Giri BS,** Geed S, Vikrant K, Lee SS, Kim KH, Kailasa SK, Vithanage M, Chaturvedi P, Rai BN, Singh RS (2021) Progress in bioremediation of pesticide residues in the environment. *Environ Eng Res* **26** https://doi.org/10.4491/eer.2020.446

[10] **Duffy KJ,** Ford RM, Cummings PT (1997) Residence time calculation for chemotactic bacteria within porous media. *Biophys. J* **73**:2930 https://doi.org/10.1016/S0006-3495(97)78321-8 | PubMed

[11] **Adadevoh JST,** Triolo S, Ramsburg CA, Ford RM (2016) Chemotaxis increases the residence time of bacteria in granular media containing distributed contaminant sources. *Environ Sci Technol* **50**:181 https://doi.org/10.1021/acs.est.5b03956 | PubMed

[12] **Adadevoh JST,** Ramsburg CA, Ford RM (2018) Chemotaxis increases the retention of bacteria in porous media with residual napl entrapment. *Environ Sci Technol* **52**:7289 https://doi.org/10.1021/acs.est.8b01172 | PubMed

[13] **De anna P,** Pahlavan AA, Yawata Y, Stocker R, Juanes R (2021) Chemotaxis under flow disorder shapes microbial dispersion in porous media. *Nat. Phys* **17**:68 https://doi.org/10.5194/egusphere-egu21-16083

[14] **Berg HC,** Turner L (1990) Chemotaxis of bacteria in glass capillary arrays. escherichia coli, motility, microchannel plate, and light scattering. *Biophys. J* **58**:919 https://doi.org/10.1016/S0006-3495(90)82436-X | PubMed

[15] **Ford RM,** Harvey RW (2007) Role of chemotaxis in the transport of bacteria through saturated porous media. *Adv. Water Resour* **30**:1608 https://doi.org/10.1016/j.advwatres.2006.05.019

[16] **Ault JT,** Shin S (2025) Physicochemical hydrodynamics of particle diffusiophoresis driven by chemical gradients. *Annu. Rev. Fluid Mech.* **57**:227 https://doi.org/10.1146/annurev-fluid-030424-110950

[17] **Park SW,** Lee J, Yoon H, Shin S (2021) Microfluidic investigation of salinity-induced oil recovery in porous media during chemical flooding. *Energy Fuels* **35**:4885 https://doi.org/10.1021/acs.energyfuels.0c04320

[18] **Doan VS,** Chun S, Feng J, Shin S (2021) Confinementdependent diffusiophoretic transport of nanoparticles in collagen hydrogels. *Nano Lett.* **21**:7625 https://doi.org/10.1021/acs.nanolett.1c02251 | PubMed

[19] **Somasundar A,** Qin B, Shim S, Bassler BL, Stone HA (2023) Diffusiophoretic particle penetration into bacterial biofilms. *ACS Appl Mater Interfaces* **15**:33263 https://doi.org/10.1021/acsami.3c03190 | PubMed

[20] **Sambamoorthy S,** Chu HCW (2023) Diffusiophoresis of a spherical particle in porous media. *Soft Matter* **19**:1131 https://doi.org/10.1039/d2sm01620f | PubMed

[21] **Jotkar M,** De Anna P, Dentz M, Cueto-Felgueroso L (2024) The impact of diffusiophoresis on hydrodynamic dispersion and filtration in porous media. *J. Fluid Mech* **991**:A8 https://doi.org/10.1017/jfm.2024.546

[22] **Jotkar M,** Ben-Noah I, Hidalgo JJ, Dentz M (2024) Diffusiophoresis of colloids in partially-saturated porous media. *Adv. Water Resour* 104828 https://doi.org/10.1016/j.advwatres.2024.104828

[23] **Alipour M,** Li Y, Liu H, Pahlavan AA (2026) Diffusiophoretic transport of colloids in porous media. *Science Advances* **12**:eady9874 https://doi.org/10.1126/sciadv.ady9874 | PubMed

[24] **Kar A,** Chiang T.-Y, Rivera IO, Sen A, Velegol D (2015) Enhanced transport into and out of dead-end pores. *ACS Nano* **9**:746 https://doi.org/10.1021/nn506216b | PubMed

[25] **Shin S,** Um E, Sabass B, Ault JT, Rahimi M, Warren PB, Stone HA (2016) Size-dependent control of colloid transport via solute gradients in dead-end channels. *Proc. Natl. Acad. Sci.* **113**:257 https://doi.org/10.1073/pnas.1511484112 | PubMed

[26] **Ault JT,** Warren PB, Shin S, Stone HA (2017) Diffusiophoresis in one-dimensional solute gradients. *Soft Matter* **13**:9015 https://doi.org/10.1039/c7sm01588g | PubMed

[27] **Shin S,** Warren PB, Stone HA (2018) Cleaning by surfactant gradients: Particulate removal from porous materials and the significance of rinsing in laundry detergency. *Phys. Rev. Appl.* **9**:034012 https://doi.org/10.1103/physrevapplied.9.034012

[28] **Tan H,** Banerjee A, Shi N, Tang X, Abdel-Fattah A, Squires TM (2021) A two-step strategy for delivering particles to targets hidden within microfabricated porous media. *Sci. Adv* **7**:eabh0638 https://doi.org/10.1126/sciadv.abh0638 | PubMed

[29] **Shi N,** Abdel-Fattah A (2021) Droplet migration into dead-end channels at high salinity enhanced by micelle gradients of a zwitterionic surfactant. *Phys. Rev. Fluids* **6**:053103 https://doi.org/10.1103/physrevfluids.6.053103

[30] **Duong DQ,** Ganguly A, Gupta A, Shin S (2026) Salt-mediated bidirectional propulsion of oil droplets in confined spaces. *Newton* **2**:100405 https://doi.org/10.1016/j.newton.2026.100405

[31] **Lee H,** Kim J, Yang J, Seo SW, Kim SJ (2018) Diffusiophoretic exclusion of colloidal particles for continuous water purification. *Lab Chip* **18**:1713 https://doi.org/10.1039/c8lc00132d | PubMed

[32] **Doan VS,** Saingam P, Yan T, Shin S (2020) A trace amount of surfactants enables diffusiophoretic swimming of bacteria. *ACS Nano* **14**:14219 https://doi.org/10.1021/acsnano.0c07502 | PubMed

[33] **Shim S,** Khodaparast S, Lai C.-Y, Yan J, Ault JT, Ralla-bandi B, Shardt O, Stone HA (2021) Co2-driven diffusiophoresis for maintaining a bacteria-free surface. *Soft Matter* **17**:2568 https://doi.org/10.1039/d0sm02023k | PubMed

[34] **Paustian JS,** Azevedo RN, Lundin S.-TB, Gilkey MJ, Squires TM (2013) Microfluidic microdialysis: Spatiotemporal control over solution microenvironments using integrated hydrogel membrane microwindows. *Phys. Rev. X* **3**:041010 https://doi.org/10.1103/physrevx.3.041010

[35] **Doan VS,** Alshareedah I, Singh A, Banerjee PR, Shin S (2024) Diffusiophoresis promotes phase separation and transport of biomolecular condensates. *Nature Commun.* **15**:7686 https://doi.org/10.1038/s41467-024-51840-6 | PubMed

[36] **Sullivan GM,** Feinn R (2012) Using effect size-or why the p value is not enough. *J. Grad. Med. Educ.* **4**:279 https://doi.org/10.4300/JGME-D-12-00156.1 | PubMed

[37] **Harwood CS,** Fosnaugh K, Dispensa M (1989) Flagellation of pseudomonas putida and analysis of its motile behavior. *J. Bacteriol* **171**:4063 https://doi.org/10.1128/jb.171.7.4063-4066.1989 | PubMed

[38] **Alirezaeizanjani Z,** Großmann R, Pfeifer V, Hintsche M, Beta C (2020) Chemotaxis strategies of bacteria with multiple run modes. *Sci. Adv* **6**:eaaz6153 https://doi.org/10.1126/sciadv.aaz6153 | PubMed

[39] **Thormann KM,** Beta C, Kühn MJ (2022) Wrapped up: the motility of polarly flagellated bacteria. *Annu. Rev. Microbiol.* **76**:349 https://doi.org/10.1146/annurev-micro-041122-101032 | PubMed

[40] **Qi Y,** Adler J (1989) Salt taxis in escherichia coli bacteria and its lack in mutants. *Proc. Natl. Acad. Sci.* **86**:8358 https://doi.org/10.1073/pnas.86.21.8358 | PubMed

[41] **Gao C,** Garren M, Penn K, Fernandez VI, Seymour JR, Thompson JR, Raina J.-B, Stocker R (2021) Coral mucus rapidly induces chemokinesis and genome-wide transcriptional shifts toward early pathogenesis in a bacterial coral pathogen. *The ISME journal* **15**:3668 https://doi.org/10.1038/s41396-021-01024-7 | PubMed

[42] **Packer HL,** Armitage JP (1994) The chemokinetic and chemotactic behavior of rhodobacter sphaeroides: two independent responses. *Journal of bacteriology* **176**:206 https://doi.org/10.1128/jb.176.1.206-212.1994 | PubMed

[43] **Deepika D,** Karmakar R, Tirumkudulu MS, Venkatesh K (2015) Variation in swimming speed of escherichia coli in response to attractant. *Archives of microbiology* **197**:211 https://doi.org/10.1007/s00203-014-1044-5 | PubMed

[44] **Zhulin I,** Armitage JP (1993) Motility, chemokinesis, and methylation-independent chemotaxis in azospirillum brasilense. *Journal of bacteriology* **175**:952 https://doi.org/10.1128/jb.175.4.952-958.1993 | PubMed

[45] **Benhamou S** (2004) How to reliably estimate the tortuosity of an animal's path:: straightness, sinuosity, or fractal dimension?. *J. Theor. Biol* **229**:209 https://doi.org/10.1016/j.jtbi.2004.03.016 | PubMed

[46] **Kamdar S,** Shin S, Leishangthem P, Francis LF, Xu X, Cheng X (2022) The colloidal nature of complex fluids enhances bacterial motility. *Nature* **603**:819 https://doi.org/10.1038/s41586-022-04509-3 | PubMed

[47] **Hyon Y,** Powers TR, Stocker R, Fu HC (2012) The wiggling trajectories of bacteria. *J. Fluid Mech* **705**:58 https://doi.org/10.1017/jfm.2012.217

[48] **Tokárová V,** Sudalaiyadum Perumal A, Nayak M, Shum H, Kašpar O, Rajendran K, Mohammadi M, Tremblay C, Gaffney EA, Martel S, *et al.* (2021) Patterns of bacterial motility in microfluidics-confining environments. *Proc. Natl. Acad. Sci.* **118**:e2013925118 https://doi.org/10.1073/pnas.2013925118 | PubMed

[49] **Park J,** Kim Y, Lee W, Pfeifer V, Muraveva V, Beta C, Lim S (2024) Bundling instability of lophotrichous bacteria. *Phys. Fluids* **36** https://doi.org/10.1063/5.0228395

[50] **Prieve DC,** Anderson JL, Ebel JP, Lowell ME (1984) Motion of a particle generated by chemical gradients. Part 2. Electrolytes. *J. Fluid Mech.* **148**:247 https://doi.org/10.1017/s0022112084002330

[51] **Prieve DC,** Roman R (1987) Diffusiophoresis of a rigid sphere through a viscous electrolyte solution. *J. Chem. Soc. Faraday Trans.* **83**:1287 https://doi.org/10.1039/f29878301287

[52] **Doan VS,** Kim D.-O, Snoeyink C, Sun Y, Shin S (2023) Shape-and orientation-dependent diffusiophoresis of colloidal ellipsoids. *Phys. Rev. E* **107**:L052602 https://doi.org/10.1103/PhysRevE.107.L052602 | PubMed

[53] **Lee S,** Lee J, Ault JT (2023) The role of variable zeta potential on diffusiophoretic and diffusioosmotic transport. *Colloid Surf A* **659**:130775 https://doi.org/10.1016/j.colsurfa.2022.130775

[54] **Akdeniz B,** Wood JA, Lammertink RGH (2023) Diffusiophoresis and diffusio-osmosis into a dead-end channel: Role of the concentration-dependence of zeta potential. *Langmuir* **39**:2322 https://doi.org/10.1021/acs.langmuir.2c03000 | PubMed

[55] **Berg HC** (2004) *E. coli in Motion* Springer.

[56] **Zylstra G,** McCombie WR, Gibson DT, Finette BA (1988) Toluene degradation by pseudomonas putida f1: genetic organization of the tod operon. *Appl Environ Microbiol* **54**:1498 https://doi.org/10.1128/aem.54.6.1498-1503.1988 | PubMed

[57] **Inoue A,** Horikoshi K (1989) A Pseudomonas thrives in high concentrations of toluene. *Nature* **338**:264 https://doi.org/10.1038/338264a0

[58] **Ramos JL,** Duque E, Gallegos MT, Godoy P, Ramos-Gonzalez MI, Rojas A, Terán W, Segura A (2002) Mechanisms of solvent tolerance in gram-negative bacteria. *Annu. Rev. Microbiol* **56**:743 https://doi.org/10.1146/annurev.micro.56.012302.161038 | PubMed

[59] **Parales RE,** Ditty JL, Harwood CS (2000) Toluene-degrading bacteria are chemotactic towards the environmental pollutants benzene, toluene, and trichloroethylene. *Appl Environ Microbiol.* **66**:4098 https://doi.org/10.1128/AEM.66.9.4098-4104.2000 | PubMed

[60] **Singh R,** Olson MS (2010) Kinetics of trichloroethylene and toluene toxicity to pseudomonas putida f1. *Environ Toxicol Chem.* **29**:56 https://doi.org/10.1002/etc.14 | PubMed

[61] **Wang X,** Lanning LM, Ford RM (2016) Enhanced retention of chemotactic bacteria in a pore network with residual napl contamination. *Environ Sci Technol.* **50**:165 https://doi.org/10.1021/acs.est.5b03872 | PubMed

Peer reviews

Reviewer #1 (Public review):

Summary:

The authors claim that bacteria are guided by diffusiophoresis. They perform experiments of bacterial motility in microfluidic channels with salt gradients. The data show that P. pudita bacteria swim towards higher sodium chloride concentrations, but there is no evidence that this is due to a diffusiophoresis.

Weaknesses:

It is well known that bacteria perform chemotaxis in salt gradients (see e.g., PNAS 86, pp. 8358-8362, 1989). The underlying mechanism based on chemoreceptors is widely accepted, but the authors do not mention this possibility. I recommend a control experiment where the chemotaxis genes are knocked out. Even if this mechanism can be ruled out, the current data show no evidence for a mechanism based on diffusiophoresis.

https://doi.org/10.7554/eLife.111881.1.sa2

Reviewer #2 (Public review):

Summary:

The authors investigate how salt gradients influence the transport of Pseudomonas putida in confined microfluidic environments. They report that salt gradients enhance directional migration, increase run persistence, and promote transport toward contaminant-rich regions. To explain these observations, the authors propose a physical steering mechanism in which differential diffusiophoretic mobilities of the cell body and flagellar bundle generate an aligning torque that reorients cells along the salt gradient.

Strengths:

The study addresses an interesting question at the interface of microbiology, complex fluids, and active matter. Their experiments suggest that salt gradients influence bacterial transport behavior and lead to more persistent, directional motion. Once confirmed, the proposed mechanism would broaden our understanding of how environmental gradients can shape microbial migration through physical interactions in addition to more traditional sensing-based pathways.

Weaknesses:

The main limitation of the current study is that the proposed steering mechanism is not directly demonstrated. The evidence for the diffusiophoretic torque is largely inferred from trajectory statistics and theoretical modeling. While the observed transport behavior is convincing, the causal link between the observed migration patterns and the proposed

reorientation mechanism remains less well established. In particular, the manuscript focuses primarily on cell trajectories and transport properties, whereas the proposed mechanism fundamentally involves changes in cell orientation. Additional evidence connecting orientation dynamics to the proposed torque mechanism would strengthen the conclusions.

A related concern is whether alternative physical mechanisms associated with the imposed salt gradients have been fully excluded. For example, weak flow-mediated effects or other hydrodynamic influences could potentially contribute to the observed transport behavior. The manuscript would benefit from a more thorough discussion of such possibilities and a clearer justification for why the proposed diffusiophoretic mechanism should be regarded as the dominant explanation.

The manuscript would also benefit from a clearer positioning within the broader literature on physically induced microbial transport and swimmer reorientation. Previous studies have demonstrated directed migration arising from rheotaxis (Marcos et al., 2012, PNAS) and viscosity-gradient-induced steering (Stehnach et al., 2021, Nature Physics). While the mechanism proposed here appears distinct, a more explicit discussion of how the present work relates to these earlier studies would help readers better understand the specific conceptual advance being made.

https://doi.org/10.7554/eLife.111881.1.sa1

Author response:

> ***Public Reviews:***
>
> ***Reviewer #1 (Public review):***
>
> *Summary:*
>
> *The authors claim that bacteria are guided by diffusiophoresis. They perform experiments of bacterial motility in microfluidic channels with salt gradients. The data show that P. putida bacteria swim towards higher sodium chloride concentrations, but there is no evidence that this is due to diffusiophoresis.*
>
> *Weaknesses:*
>
> *It is well known that bacteria perform chemotaxis in salt gradients (see e.g., PNAS 86, pp. 8358-8362, 1989). The underlying mechanism based on chemoreceptors is widely accepted, but the authors do not mention this possibility. I recommend a control experiment where the chemotaxis genes are knocked out. Even if this mechanism can be ruled out, the current data show no evidence for a mechanism based on diffusiophoresis.*

We thank the reviewer for raising this important comment. We agree that receptor-mediated salt taxis is a well-established mechanism in some bacteria, including the classic study by Qi and Adler (PNAS, 1989). We note, however, that the original manuscript did discuss this possibility and cited Qi and Adler in line 117: “We also note that we did not observe any significant difference in the tumble rates between the control and NaCl gradient cases (Figure 3h; Figure S2, SM), suggesting that NaCl gradients do not interfere with chemoreceptors (Qi and Adler, 1989).” In Figure S2, the run-time distributions show no significant difference between the no-gradient condition and the NaCl-gradient condition, with fitted tumble rates of $\lambda = 0.41\ s^{-1}$ and $\lambda = 0.38\ s^{-1}$, respectively. We also do not observe a directional bias in run duration, namely longer runs up the salt gradient and shorter runs down the gradient, which would be expected for canonical chemoreceptor-mediated taxis.

The basis for assigning the observed migration to diffusiophoresis is that the NaCl gradient produces a directional drift of the bacterial body without a measurable change in the run-

and-tumble statistics. This behavior is consistent with our previous work [1], where non-motile bacteria were shown to undergo diffusiophoretic migration toward higher salt concentration. Because that migration occurred in non-motile cells and across different bacterial types and morphologies, it supports the interpretation that native bacterial surface charge can drive a non-specific diffusiophoretic response in salt gradients.

That said, we agree with the reviewer that a genetic control would provide a stronger test against receptor-mediated chemotaxis. We will therefore perform additional experiments using a ΔcheA strain. Because CheA is required for canonical chemotactic signal transduction, observing the same directional migration in the ΔcheA mutant would directly test whether the NaCl gradient response persists in the absence of receptor-mediated chemotaxis. We will include these new data and revise the manuscript to more explicitly distinguish diffusiophoretic drift from chemoreceptormediated salt taxis.

> ***Reviewer #2 (Public review):***
>
> *Summary:*
>
> *The authors investigate how salt gradients influence the transport of Pseudomonas putida in confined microfluidic environments. They report that salt gradients enhance directional migration, increase run persistence, and promote transport toward contaminant-rich regions. To explain these observations, the authors propose a physical steering mechanism in which differential diffusiophoretic mobilities of the cell body and flagellar bundle generate an aligning torque that reorients cells along the salt gradient.*
>
> *Strengths:*
>
> *The study addresses an interesting question at the interface of microbiology, complex fluids, and active matter. Their experiments suggest that salt gradients influence bacterial transport behavior and lead to more persistent, directional motion. Once confirmed, the proposed mechanism would broaden our understanding of how environmental gradients can shape microbial migration through physical interactions in addition to more traditional sensing-based pathways.*
>
> *Weaknesses:*
>
> *The main limitation of the current study is that the proposed steering mechanism is not directly demonstrated. The evidence for the diffusiophoretic torque is largely inferred from trajectory statistics and theoretical modeling. While the observed transport behavior is convincing, the causal link between the observed migration patterns and the proposed reorientation mechanism remains less well established. In particular, the manuscript focuses primarily on cell trajectories and transport properties, whereas the proposed mechanism fundamentally involves changes in cell orientation. Additional evidence connecting orientation dynamics to the proposed torque mechanism would strengthen the conclusions.*

We thank the reviewer for the constructive comments. We agree that the proposed steering mechanism should be supported by evidence that directly connects the salt gradient response to bacterial orientation dynamics, not only to trajectory-level transport statistics.

We would like to clarify that the original manuscript already includes an orientation-based analysis in Figure 4f,g in the main text. The corresponding methodology and results are described in lines 173–183 and in the Supporting Information. Specifically, we quantified cell steering by measuring the change in body angle, $\Delta\theta$, along individual run trajectories as a function of arc length, s, using the orientation correlation $\langle\cos(\Delta\theta)\rangle_s$. In the absence of salt gradients, the orientation correlation decays slowly with arc length, indicating persistent swimming along the initial

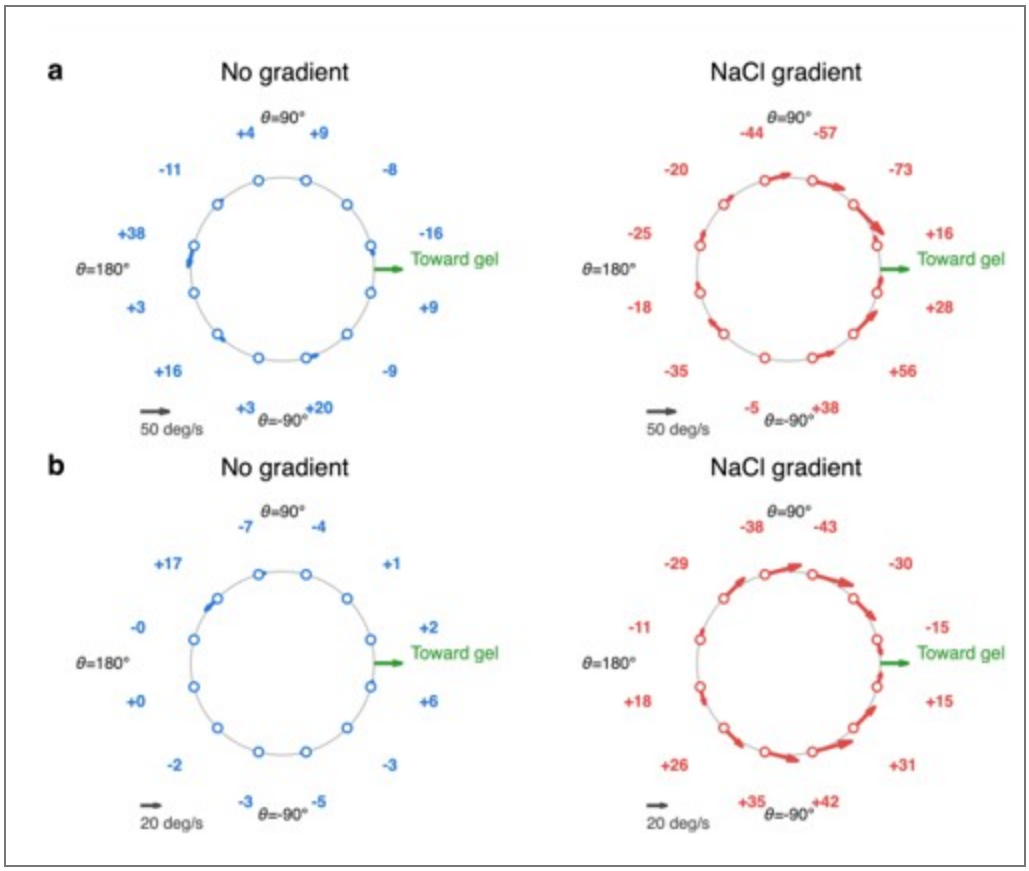

Author response image 1. Instantaneous angular velocity as a function of heading angle relative to the salt gradient orientation. (a) Experimental and (b) simulated mean angular velocity of cells as a function of heading angle θ (measured relative to the gradient direction; θ = 0° points toward the gel/high-salt side) in the absence (blue) and presence (red) of a NaCl gradient. Positive and negative values indicate counterclockwise and clockwise rotation, respectively, with arrows showing rotation direction. Under the gradient, both experiments and simulations show a signed, angle-dependent rotation rate that is largest near θ = ±90° and approaches zero near θ = 0° and 180°, consistent with a restoring torque that steers cell heading toward the gradient direction. Simulations reproduce this behavior with comparable magnitude to the experimental measurements, and in the absence of a gradient, angular velocity remains relatively small in the no-gradient case with no consistent directional bias across heading angles.

run direction. Under a salt gradient, the correlation decays more rapidly, indicating stronger directional reorientation during runs. Because the tumble statistics do not change significantly between the no-gradient and salt-gradient conditions, this enhanced orientational decorrelation is not attributed to increased tumbling or rotational noise. Instead, it is consistent with continuous deterministic steering during runs, as expected from a diffusiophoretic torque acting on the cell body–flagellar bundle system.

To further address the reviewer's concern, we performed an additional orientation-dynamics analysis using the same dataset shown in Figure 4. Following the approach used by Stehnach et al. [2], we calculated the instantaneous angular velocity during individual runs as a function of the cell heading angle relative to the salt gradient direction. The cell orientation was obtained from the run trajectories, and tumble events were excluded because they produce large transient angular velocity spikes that are not representative of continuous steering during runs.

The new analysis is shown in Author response image 1. Under the no-gradient condition, the angular velocity remains small and nearly independent of heading angle. In contrast, under the salt gradient condition, the angular velocity becomes strongly heading-dependent. The

angular velocity is largest when cells swim nearly perpendicular to the salt gradient, where a steering torque is expected to be maximal. Moreover, the sign of the angular velocity indicates rotation toward alignment with the gradient direction. This behavior is consistent with the proposed diffusiophoretic torque mechanism and provides a direct link between the observed transport behavior and salt-gradient-induced reorientation dynamics.

We plan to add this angular velocity analysis to the revised manuscript and revise the relevant text to make the connection between trajectory statistics, orientation dynamics, and the proposed torque mechanism clearer.

> *A related concern is whether alternative physical mechanisms associated with the imposed salt gradients have been fully excluded. For example, weak flow-mediated effects or other hydrodynamic influences could potentially contribute to the observed transport behavior. The manuscript would benefit from a more thorough discussion of such possibilities and a clearer justification for why the proposed diffusiophoretic mechanism should be regarded as the dominant explanation.*

We thank the reviewer for raising this important point. We agree that alternative physical mechanisms associated with the imposed salt gradient should be considered explicitly. In the revised manuscript, we will add a more detailed discussion explaining why flow-mediated or other hydrodynamic mechanisms are unlikely to account for the observed steering behavior.

First, the characteristic diffusiophoretic drift velocity in our experiments is approximately $u_d \approx 1$ μm/s, corresponding to only about 1–5% of the typical swimming speed of P. putida. Thus, the proposed mechanism does not require externally driven advection of the cells. Instead, the salt gradient produces a weak but persistent differential diffusiophoretic slip on the cell body and flagellar bundle, which can generate a reorienting torque during active swimming.

We also considered whether diffusio-osmotic flow along the channel walls could generate sufficient shear to induce rheotaxis. In a dead-end channel, the diffusio-osmotic velocity profile can be estimated as [3]

$$v_z(x,z) = \frac{\Gamma_w}{2}\frac{d^2 \ln c}{dx^2}\left[z\left(\left(\frac{z}{h}\right)^2 - 1\right)\right] \tag{1}$$

which gives a wall shear rate (at $z = h$) of

$$\dot{\gamma}_{\text{wall}} = \Gamma_w \left|\frac{d^2 \ln c}{dx^2}\right| \sim 0.01 - 0.04\ \text{s}^{-1}. \tag{2}$$

This value is below the shear rate threshold reported by Marcos et al. [2], where rheotactic drift becomes negligible for $S < 0.1\ \text{s}^{-1}$. Therefore, the shear generated by diffusio-osmotic wall flow in our experiments is too weak to explain the observed directional reorientation. This effect would be even smaller for P. putida, whose thin flagellar bundle is expected to experience weaker shear-induced alignment than organisms with larger flagellar structures.

We further considered viscotaxis as a possible mechanism. However, the viscosity difference between 1 mM and 100 mM NaCl solutions is marginal. This contrast is far smaller than the approximately 4–5-fold viscosity difference reported to induce strong viscophobic turning in bacteria [4]. Thus, salt-gradient-induced viscosity variations are insufficient to account for the measured steering response.

Taken together, these estimates indicate that hydrodynamic shear, rheotaxis, and viscotaxis are too weak under our experimental conditions to explain the observed migration and orientation dynamics. In contrast, the proposed nonuniform diffusiophoretic mechanism

naturally accounts for the key observations: directional migration up the salt gradient, enhanced curvature during runs, heading-dependent angular velocity, and the absence of significant changes in tumble statistics. We will include this analysis in the revised manuscript to clarify why diffusiophoretic steering is the dominant mechanism under the present conditions.

> *The manuscript would also benefit from a clearer positioning within the broader literature on physically induced microbial transport and swimmer reorientation. Previous studies have demonstrated directed migration arising from rheotaxis (Marcos et al., 2012, PNAS) and viscosity-gradient-induced steering (Stehnach et al., 2021, Nature Physics). While the mechanism proposed here appears distinct, a more explicit discussion of how the present work relates to these earlier studies would help readers better understand the specific conceptual advance being made.*

We thank the reviewer for this helpful suggestion. We agree that the manuscript should more clearly position the proposed mechanism within the broader literature on physically induced microbial transport and swimmer reorientation.

In the revised manuscript, we have added a discussion comparing our results with prior studies on rheotaxis and viscosity-gradient-induced steering. Specifically, we now discuss the work of Marcos et al. [4], which showed that shear flow can generate a torque on the helical flagellum of Bacillus subtilis, producing rheotactic alignment independent of chemical sensing. We also discuss the work of Stehnach et al. [2], which showed that viscosity gradients can steer Chlamydomonas reinhardtii through asymmetric viscous drag on its two flagella, producing viscophobic turning down the viscosity gradient.

The mechanism proposed in the present work is distinct from both of these cases. Unlike rheotaxis, it does not require externally imposed shear flow. Unlike viscophobic turning, it does not rely on a substantial viscosity contrast. Instead, we propose that a salt concentration gradient generates differential diffusiophoretic motion of the cell body and flagellar bundle, producing a torque that continuously reorients swimming cells along the gradient. This mechanism therefore identifies salt gradients as a distinct physical cue capable of steering bacteria through surface-mediated transport rather than through flow, viscosity contrast, or canonical chemoreceptor signaling.

We have added the following text to the revised manuscript: ”Our findings also relate to other physical mechanisms of microbial reorientation. Bacterial rheotaxis, arising from a torque generated by shear flow acting on the helical flagellum, steers Bacillus subtilis independent of any chemical gradient [4]. Viscosity gradients similarly drive a viscophobic turning in the alga Chlamydomonas reinhardtii, where uneven viscous drag on its two flagella produces a torque that reorients cells down the gradient [2], a behavior confirmed by measuring angular velocity as a function of heading angle and revealing a sinusoidal form, $\omega(\theta) = -\omega_{\mathrm{visc}} \sin(\theta)$, which resembles what we report here for diffusiophoresis in (Figure S4). This identifies salt gradients, independent of flow or viscosity, as a distinct physical route by which swimming cells can be steered and guided, broadening the set of known nonchemoreceptor mechanisms for directed microbial transport.” References

(1) V. S. Doan, P. Saingam, T. Yan, S. Shin, A trace amount of surfactants enables diffusiophoretic swimming of bacteria, ACS Nano 14 (10) (2020) 14219–14227.

(2) M. R. Stehnach, N. Waisbord, D. M. Walkama, J. S. Guasto, Viscophobic turning dictates microalgae transport in viscosity gradients, Nature Physics 17 (8) (2021) 926–930.

(3) S. Shin, E. Um, B. Sabass, J. T. Ault, M. Rahimi, P. B. Warren, H. A. Stone, Size-dependent control of colloid transport via solute gradients in dead-end channels, Proc. Natl. Acad. Sci. 113 (2) (2016) 257–261.

(4) Marcos, H. C. Fu, T. R. Powers, R. Stocker, Bacterial rheotaxis, Proceedings of the National Academy of Sciences 109 (13) (2012) 4780–4785.

https://doi.org/10.7554/eLife.111881.1.sa0